Oncogene (2010) 29, 3435–3445

www.nature.com/onc

ORIGINAL ARTICLE

The immortalizing and transforming ability of two common human papillomavirus 16 E6 variants with different prevalences in cervical cancer

C Richard[1], C Lanner[2], SN Naryzhny[3,4], L Sherman[5], H Lee[2,4], PF Lambert[6] and I Zehbe[7]

[1]Research Laboratory, Thunder Bay Regional Health Sciences Centre, Thunder Bay, Ontario, Canada; [2]Molecular Genetics, Northern Ontario School of Medicine, Laurentian University, Sudbury, Ontario, Canada; [3]Department of Chemistry and Biochemistry, Laurentian University, Sudbury, Ontario, Canada; [4]Northeastern Ontario Regional Cancer Program at Sudbury Regional Hospital, Sudbury, Ontario, Canada; [5]Department of Clinical Microbiology and Immunology, Sackler School of Medicine, Tel-Aviv University, Tel-Aviv, Israel; [6]McArdle Laboratory for Cancer Research, University of Wisconsin, Madison, WI, USA and [7]Probe Development and Biomarker Exploration, Thunder Bay Regional Research Institute, Thunder Bay, Ontario, Canada

Persistent infection with high-risk human papillomaviruses (HPVs), especially type 16 has been undeniably linked to cervical cancer. The Asian-American (AA) variant of HPV16 is more common in the Americas than the prototype in cervical cancer. The different prevalence is based on three amino acid changes within the E6 protein denoted Q14H/H78Y/L83V. To investigate the mechanism(s) behind this observation, both E6 proteins, in the presence of E7, were evaluated for their ability to extend the life span of and transform primary human foreskin keratinocytes (PHFKs). Long-term cell culture studies resulted in death at passage 9 of vector-transduced PHFKs (negative control), but survival of both E6 PHFKs to passage 65 (and beyond). Compared with E6/E7 PHFKs, AA/E7 PHFKs were significantly faster dividing, developed larger cells in monolayer cultures, showed double the epithelial thickness and expressed cytokeratin 10 when grown as organotypic raft cultures. Telomerase activation and p53 inactivation, two hallmarks of immortalization, were not significantly different between the two populations. Both were resistant to anoikis at later passages, but only AA/E7 PHFKs acquired the capacity for *in vitro* transformation. Proteomic analysis revealed markedly different protein patterns between E6/E7 and AA/E7, particularly with respect to key cellular metabolic enzymes. Our results provide new insights into the reasons underlying the greater prevalence of the AA variant in cervical cancer as evidenced by characteristics associated with higher oncogenic potential.

Oncogene (2010) **29,** 3435–3445; doi:10.1038/onc.2010.93; published online 12 April 2010

Keywords: human papillomavirus; human primary foreskin keratinocytes; immortalization; transformation; cervical cancer

Correspondence: Dr I Zehbe, Probe Development and Biomarker Exploration, Thunder Bay Regional Research Institute, 980 Oliver Road, Thunder Bay, Ontario, Canada P7B 6V4.
E-mail: zehbei@tbh.net
Received 8 September 2009; revised 23 November 2009; accepted 24 February 2010; published online 12 April 2010

Introduction

The human papillomaviruses (HPVs) comprise over 100 numerically designated genotypes, of which types 16 and 18 cause the vast majority of cervical cancer worldwide (Castellsague, 2008). Further diversity arises within any given HPV genotype through limited nucleotide changes in the coding (at a frequency of $<2\%$) and non-coding (at a frequency of $<5\%$) regions (Bernard *et al*., 2006). Such variants phylogenetically segregate based on their geographical origin and are therefore labeled European, African, Asian, Asian-American (AA) and North American. Significant differences in pathogenicity exist between variants within a single genotype. These differences have been elucidated most clearly for HPV16. Multiple studies have shown that HPV16 variants differ in their association with cervical cancer (Tidy *et al*., 1989; Berumen *et al*., 2001; Zehbe *et al*., 1998a, b, 2001; Kammer *et al*., 2002; Xi *et al*., 2007), viral persistence (Grodzki *et al*., 2006; Xi *et al*., 2006; Lee *et al*., 2008) and the frequency of recurrence of cervical disease (Xi *et al*., 2007). Increased risk of anal cancers has also been reported for certain HPV16 variants (Xi *et al*., 1998). Genomic variation and a 2 00 000 year evolutionary timeline have been presented as reasons why HPV16 is the most prevalent HPV genotype in cervical and other human cancers (Bernard, 2005).

A majority of the functional and mechanistic studies on HPV16 have been carried out using the prototype of the transforming early-expressed protein, E6 (reviewed in Seedorf *et al*., 1985; Zehbe *et al*., 1998a), while only five studies have looked at HPV16 E6 variants (Stöppler *et al*., 1996; Chakrabarti *et al*., 2004; Lichtig *et al*., 2006; Asadurian *et al*., 2007; Zehbe *et al*., 2009). The HPV16 E6 prototype and variants differ in their: binding to the calcium-binding protein, E6-PB (Lichtig *et al*., 2006), an E6 target involved in differentiation, activities in abrogating serum/calcium-induced differentiation (Asadurian *et al*., 2007), expression of cytokeratins in organotypic cultures (Zehbe *et al*., 2009) and transformation of a spontaneously immortalized aneuploid human keratinocyte cell line, (HaCaT; described by Boukamp *et al*., 1988) (Chakrabarti *et al*., 2004).

A non-European, naturally occurring E6 variant of HPV16—the AA variant—is found up to 20 times more often in cervical cancer in the Americas than the prototype (Xi *et al*., 1997; Berumen *et al*., 2001, 2007). Compared with HPV16 prototype, AA differs by three amino acid changes within its E6 protein denoted Q14H/H78Y/L83V. Interestingly, amino acid changes at positions 14 and 83 were found to be under Darwinian selective pressure (Chen *et al*., 2005). On the basis of the predicted structural HPV16 E6 model, these residues are buried, there by effecting the stability and function of the E6 protein (Nomine *et al*., 2006). Two nonexclusive mechanisms may explain the greater association of the AA variant with cervical cancer: more efficient evasion of host immune surveillance and increased oncogenic potential (Zehbe *et al*., 2003; de Araujo Souza *et al*., 2009).

In this study, we wished to test the hypothesis that the AA variant has increased oncogenic potential, and in doing so, shed light on the mechanisms behind AA's increased pathogenicity. Specifically, we compared the abilities of the prototype and AA E6 proteins to extend the life span (immortalize) and transform long-term cultures of primary human foreskin keratinocytes (PHFKs) in the presence of the E7 oncoprotein that is normally co-expressed with E6 in cervical cancers.

Results

AA/E7- and E6/E7-transduced PHFKs differ in their proliferation potential and epithelial differentiation profile

PHFKs have a limited lifespan, undergo senescence (crisis) and eventually die. The E6 protein of high-risk HPV, in the presence of E7, is known to overcome initial crisis and lead cells into immortalization (Kaur and McDougall, 1989). What was unknown was whether the HPV16 AA variant, in conjunction with the HPV16 E7 protein, is a more powerful immortalizing agent than is the HPV16 prototype E6/E7. The endpoint of our immortalization study was 65 passages, which is well accepted to represent an infinite life span (Boukamp *et al*., 1988; Woodworth *et al*., 1988; Shen *et al*., 2004). The expression of prototype and variant HPV16 E6 genes as well as the HPV16 E7 prototype gene was higher at endpoint passage 65 than at early, that is, passage 6, which is in concordance to what has been reported previously for E6 (Fu *et al*., 2003) (Figure 1).

As a result of repressing the tumor suppressor protein retinoblastoma by E7, the cyclin-dependent kinase inhibitor p16 is overexpressed in cervical cancer. As expected, we found western blot levels of p16 to be similarly high in the two populations between passages 16 and 65 while the negative control, vector-transduced PHFKs contained barely detectable amounts of p16 (Figure 2). This illustrates that E7 has similar effects in both prototype E6/E7- and AA/E7-transduced keratinocytes and that differences noted between the two populations are caused by the differences between the E6 proteins.

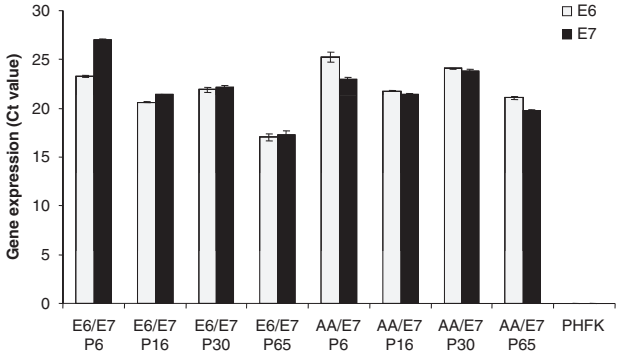

Figure 1 Relative levels of HPV16 E6 and E7 messenger RNA. The gene expression of E6 and E7 at different passages, as defined by quantitative reverse transcriptase (qRT)–PCR, is shown in PHKFs that have been retrovirally transduced with both viral oncogenes—E6 (prototype or AA) and E7. Values are expressed as Ct and have been normalized to total RNA input because the values were above those obtained for the housekeeping gene HPRT1—the most suitable normalizing gene for keratinocytes (DeCarlo *et al*., 2008). Please note that the higher the Ct value the lower is the actual gene expression. PHFKs with the empty vector were negative controls. The values of three independent experiments for each cell transduction are shown.

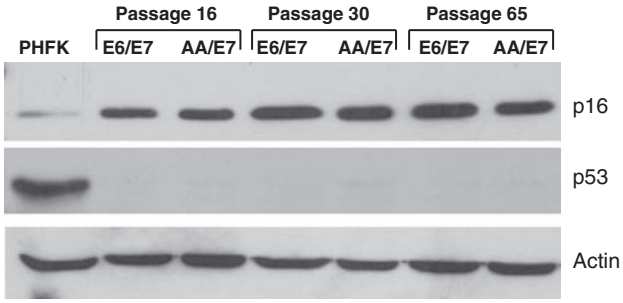

Figure 2 Protein levels of p16 and p53. Western blot protein expression is shown for passage 16, 30 and 65 in parental, E6/E7- and AA/E7-transduced PHFKs. Actin was used as loading positive control. Data shown are representative of three experiments.

AA/E7-transduced PHFKs were first to reach the endpoint of passage 65, after 403 days in culture. E6/E7-transduced PHFKs, on the other hand, needed 522 days to reach passage 65 (Figure 3a) with the difference being highly statistically significant ($P > 0.0001$; average = 290.45/s.d. = 141.26 and average = 220.93/s.d. = 105.16 for E6/E7 and AA/E7 PHFKs, respectively). All cultures underwent a crisis at around passage 9–10. PHFKs transduced with the empty vector died at passage 9 (data not shown). The doubling times (hours) of the AA/E7 PHFKs at the time of crisis were reproducibly shorter than those of the E6/E7 PHFKs in three independently transduced populations ($P = 0.02$; average = 278.39/s.d. = 50.42 and average = 150.03/s.d. = 19.86 for E6/E7 and AA/E7 PHFKs, respectively) (Figure 3b). This shortened crisis period doubling time contributed, in part, to the AA/E7 populations reaching the endpoint sooner.

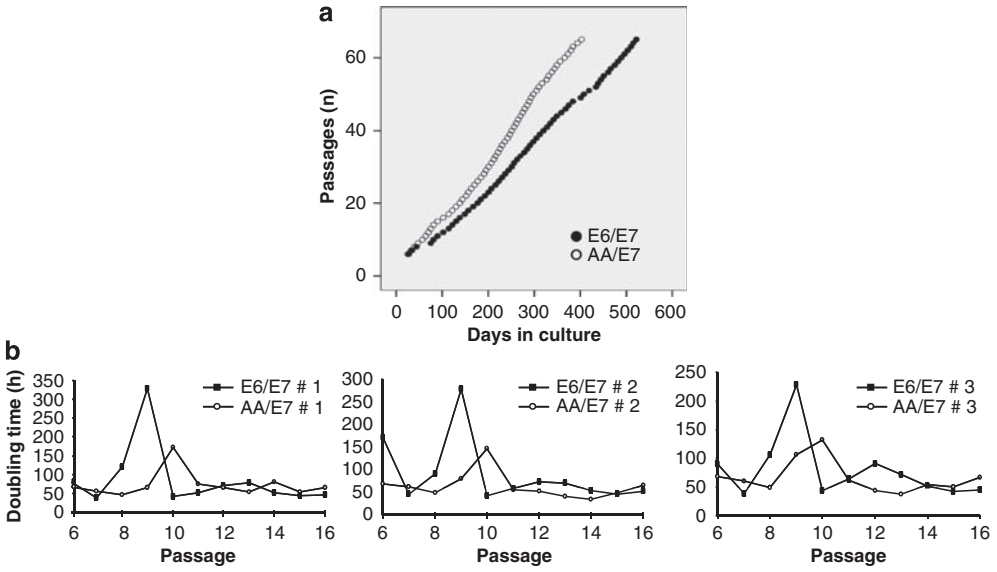

Figure 3 Proliferation profile. (**a**) The number of passages compared with days in culture for HPV16 E6/E7- and AA/E7-transduced PHFKs is shown. Each circle represents one passage. We passaged replicates of each gene set— E6/E7 or AA/E7 at the same time as they did not differ significantly in growth potential. An equal amount of cells (0.125×10^6) was plated each time. The Wilcoxon signed-rank test was used for statistical analysis. (**b**) The growth curve of triplicate lines of HPV16 E6/E7- and AA/E7-transduced PHFKs is shown individually in a diagram for passages 6 to 16. The Fisher's exact test was used for statistical analysis.

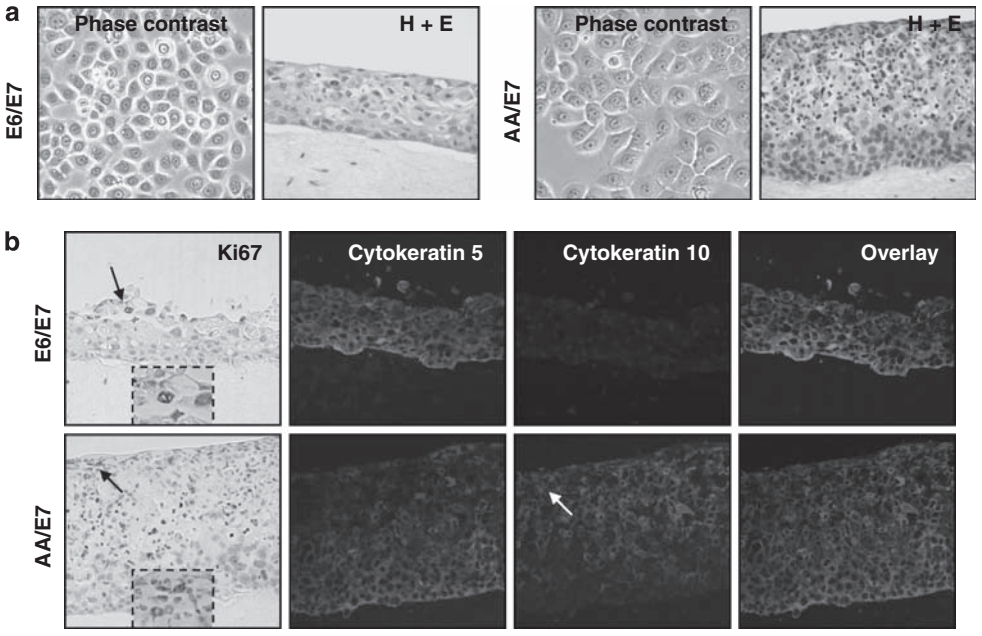

Figure 4 Monolayer and organotypic raft cultures. (**a**) Phase-contrast imaged monolayer cultures and hematoxylin and eosin stained raft cultures from passage 65 E6/E7 and AA/E7 PHFKs are shown. (**b**) Serial sections were used for immunostainings against Ki67 and cytokeratins 5 and 10. Left panel: bright-field microscopy showing Ki67 staining. Positive signals in nuclei appear in brown because of 3,3′-diaminobenzidine precipitate. The inlet shows the magnification of the area centered round the arrow with Ki67-positive cells. Middle panels: double fluorescence microscopy showing cytoplasmic cytokeratin 5 (green) and cytokeratin 10 (red) staining. Right panel: overlay. Cells expressing both cytokeratin 5 and 10 appear in yellow. Rafts were grown in triplicate. Original magnification was $\times 200$. A full colour version of this figure is available at the *Oncogene* journal online.

Not only did the AA/E7 PHFKs pass through crisis quicker than E6/E7-transduced populations, but they also had overall faster doubling times post-crisis (significant for passages 11–63: $P = 0.037$; average = 49.77/s.d. = 12.63 and average = 45.57/s.d. = 10.91 for E6/E7 and AA/E7 PHFKs, respectively), which also contributed to AA/E7 populations reaching the endpoint sooner than E6/E7 populations. Variant AA/E7 PHFKs had larger cell morphology than did prototype E6/E7-tranduced PHFKs when grown on plastic (Figure 4a). In three-dimensional

organotypic raft cultures, the AA/E7 populations reached an epithelial thickness at least twice that of prototype E6/E7 cultures (Figure 4a), consistent with the variant AA/E7 populations being more hyperplastic than the prototype E6/E7 populations. Both AA/E7 and E6/E7 populations showed epithelial changes in raft cultures comparable to a high-grade squamous intraepithelial lesion. Only AA/E7 showed suprabasal epithelial layers consisting of highly keratinized and atypical cells. Ki67, a marker to determine the growth fraction of a given cell population (Schonk *et al*., 1989) was observed in single cells within the lower, and interestingly, also the upper (keratinizing) part of the AA/E7 raft epithelium, as well as in single cells of the E6/E7 raft epithelium (Figure 4b). Although differentiation-associated cytokeratin 10 (K10), was found in the majority of suprabasal cells within the AA/E7 culture, the E6/E7 culture was devoid of any K10 staining (Figure 4b). Proliferation-associated K5, which normally is present in basal cell layers of normal stratified squamous epithelium (Zehbe *et al*., 2009) was expressed within all cells of the E6/E7 raft epithelium. In the AA/E7 raft, K5 was detected within all cells of the lower half of and within a subset of cells of the upper half of the epithelium, with consequent overlapping of K5 and K10 expression (Figure 4b). It is noteworthy that a subset of Ki67-positive cells was found in an area of K10-positive cells within the upper part of the AA/E7 raft (white arrow in Figure 4b).

Telomerase activation and p53 inactivation are similar in the E6/E7 and AA/E7 cultures

Telomerase activation and p53 inactivation, and with that the onset of genomic instability are two important events in carcinogenesis (Hanahan and Weinberg, 2000). The E6 protein of high-risk HPV induces cellular telomerase activity (Klingelhutz *et al*., 1996) and degrades p53 (Huibregtse *et al*., 1991), the latter through ubiquitin-dependent (Scheffner *et al*., 1993) and ubiquitin-independent mechanisms (Camus *et al*., 2007). Telomerase activation (Klingelhutz *et al*., 1996) and p53 inactivation (Dalal *et al*., 1996; McMurray and McCance, 2004) have both been implicated as mechanisms by which the E6 protein induces immortalization of human epithelial cells.

We carried out biochemical studies to determine if the differences between the E6 prototype and variant protein lie at the level of telomerase induction. Telomerase activity correlates with levels of hTERT messenger RNA (Kyo *et al*., 1999; Sumida *et al*., 1999; Shamanin *et al*., 2008), which is the rate-limiting determinant of the enzymatic activity of telomerase (Kyo *et al*., 1999). Consequently, we measured hTERT messenger RNA levels using quantitative reverse transcriptase–PCR (Kirkpatrick *et al*., 2004, Sekaric *et al*., 2008) based on sensitive and specific Taqman chemistry previously optimized in our laboratory (DeCarlo *et al*., 2008). We found hTERT expression to be lowest (and at the same levels) at passage 6 for the negative control, E6/E7, and AA/E7 cultures. E6 alone induces telomerase expression and activity modestly, with further increases observed once cells have undergone crisis (Sprague *et al*., 2002; James *et al*., 2006). The levels of hTERT in the E6/E7- and AA/E7-transduced cultures increased steadily, peaking at passage 65 (Figure 5). Statistically significant differences were noted at passages 16, 30 and 65 compared with parental PHFKs, but not between the E6/E7 and AA/E7 populations.

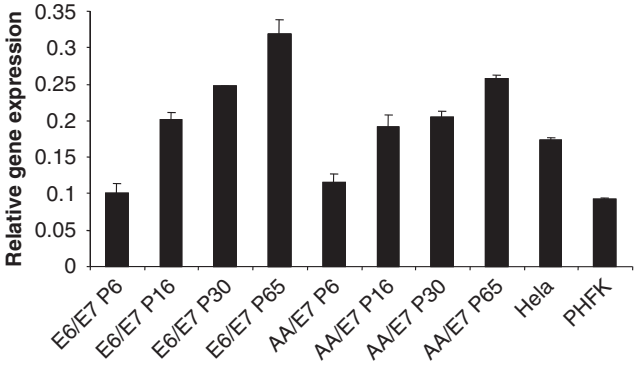

Figure 5 hTERT transcription levels. The relative expression of hTERT messenger RNA by quantitative reverse transcriptase (qRT)–PCR of HPV16 E6/E7- and AA/E7-transduced PHFKs is shown for passages 6, 16, 30 and 65, as well as for HeLa cells (positive control) and parental PHFKs (negative control). Values were normalized to the housekeeping gene HPRT1. The numbers are averages/s.d.s of three independent experiments. The Student's *t*-test was used for statistical analysis.

We functionally characterized the degree to which prototype or variant HPV16 E6 proteins inactivate p53, another target of E6 implicated in immortalization. Western blots were performed at passages 16, 30 and 65. Levels of total p53 protein in this study were similarly undetectable in both the E6/E7 and AA/E7 PHFK cultures at all passages tested, while early passage parental PHFKs showed strong expression levels (Figure 2). We also compared the capacity of the HPV16 prototype and AA E6 proteins to overcome DNA damage-induced inhibition of DNA synthesis and cell cycle arrest, two activities correlating with E6's ability to inactivate p53 (Song *et al*., 1998). Cells were treated with actinomycin D (AD) followed by cell cycle analysis. Both E6/E7 and AA/E7 cultures overcame G1 arrest after AD treatment at passages 16, 30 and 65 and showed a significantly higher resistance than the parental control keratinocytes, which showed G1 arrest when treated with AD (Figure 6a). The G1/S ratio of the AD and untreated samples of the prototype and AA E6-transduced keratinocytes ranged between 0.64 and 1.1 (mean values of the passages tested; not significantly different) while the G1/S ratio of vector-transduced keratinocytes was approximately 2.5 and significantly different from E6/E7 and AA/E7 PHFKs (Figure 6b).

Resistance to detachment-induced cell death (anoikis) is similar in E6/E7 and AA/E7 cells but only AA/E7 cells show signs of transformation in vitro

In vivo, when detached from the basal membrane, primary keratinocytes are committed to anoikis,

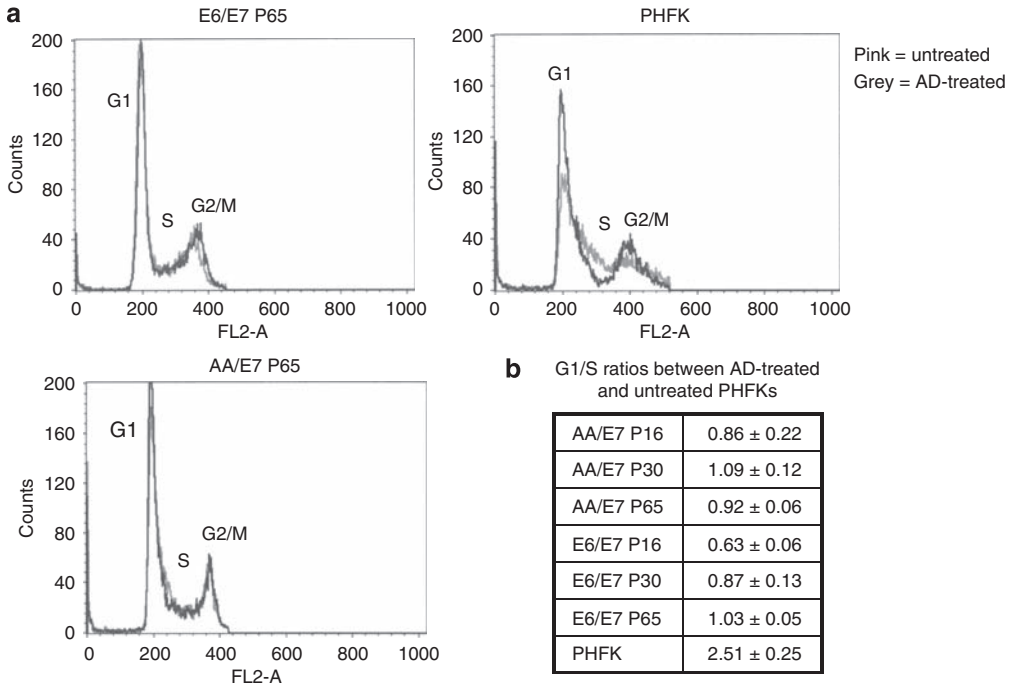

AA/E7 P16	0.86 ± 0.22
AA/E7 P30	1.09 ± 0.12
AA/E7 P65	0.92 ± 0.06
E6/E7 P16	0.63 ± 0.06
E6/E7 P30	0.87 ± 0.13
E6/E7 P65	1.03 ± 0.05
PHFK	2.51 ± 0.25

Figure 6 DNA damage-induced cell cycle arrest. The cell cycle profiles of parental PHFKs as well as HPV16 E6/E7- and AA/E7-transduced PHFKs at passage 65 are shown with and without AD treatment (0.5 nM for 24 h). (**a**) The DNA histogram, as measured by flow cytometry, shows the distribution of cells in the G1, S and G2/M phases of the cell cycle. (**b**) The G1/S ratios between the AD-treated and untreated PHFKs are shown. The numbers are averages/s.d.s of three independent experiments. The Student's *t*-test was used for statistical analysis. A full colour version of this figure is available at the *Oncogene* journal online.

terminal differentiation followed by programmed cell death. Anoikis is triggered by the extrinsic death receptor pathway (Marconi *et al*., 2004), and it can be reproduced in the laboratory by plating cells in semi-solid medium. During oncogenesis, transformed cells are much less prone to undergo apoptosis and can survive detachment from the basal membrane (or substrate).

Compared with keratinocytes transduced with vector alone, E6/E7 and AA/E7 cultures were significantly more resistant to apoptosis when grown in semi-solid medium (Figure 7). This resistance was enhanced to the same extent in both cultures at passage 30. Although the E6/E7 culture seemed more resistant than the AA/E7 culture at passage 65, these differences were not statistically significant. Thus, detachment/anchorage-independent survival was comparable between E6/E7 and AA/E7 PHFKs.

Anchorage-independent growth is considered the most accurate and stringent *in vitro* assay to detect fully transformed cells (Androphy *et al*., 1985). This has been reported to occur at low efficiency in human fetal esophageal epithelial cells in the presence of HPV18 E6/E7 at passage 65 (Shen *et al*., 2004). In this study, passage 65 E6/E7 and AA/E7 cultures were assessed for their ability to form colonies when grown in semi-soft agar. Rather than resorting to the traditional, subjective method of manually counting and estimating the size of colonies (Hahn *et al*., 1999), we used an assay that allowed additional quantification (described in detail in the Materials and methods section). The AA/E7 PHFKs and HeLa cells (positive control) showed colony growth after 10 days. In contrast, the E6/E7 prototype culture and the negative control cells (parental PHFKs) were unable to produce colony growth (Figure 8). This observation was confirmed by quantifying cell transformation as determined by cell viability using the 3-(4,5-dimethylthiazol-2-yl)-2,5-diphenyltetrazolium bromide (MTT) assay (Figure 8).

Host cellular proteins associated with metabolic enzymes are differentially expressed in E6/E7- and AA/E7-transduced keratinocytes

To identify possible E6 targets for the differences observed in the immortalization and transforming ability, we performed proteomics analyses using two-dimensional gel electrophoresis and matrix-assisted laser desorption/ionization mass spectroscopy on the passage 65 E6/E7 and AA/E7 PHFKs, as well as on parental PHFKs.

We compared data acquired from three independent two-dimensional gel electrophoresis experiments. The average spot number per gel set ranged from 371 to 383 and a total of 564 spots from all the gels were present in the final master composite (Table 1). Using the software PD Quest (Bio-Rad Laboratories, Hercules, CA, USA), a total of 28 protein spots that were expressed at significantly different levels in at least two of the pair-wise comparisons between the cell types were identified. Six of the protein spots were indistinct and not identifiable. Of the 22 cut spots, 14 spots revealed proteins that were similarly expressed between E6/E7 and AA/E7 gels, but differed in intensity from parental

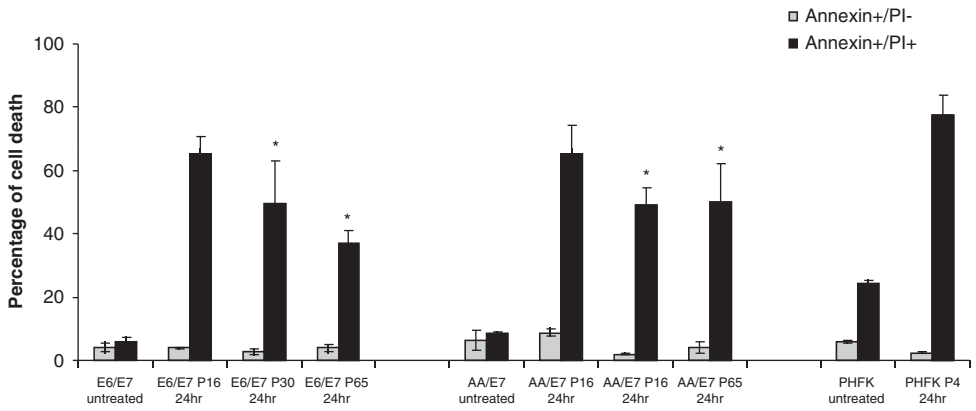

Figure 7 The ability to resist cell death. PHFKs were grown in semi-solid (ss) medium for 24 h at passage 16, 30 and 65. Using flow cytometry, early apoptotic (annexin V-FITC + /PI–) and late apoptotic (annexin V-FITC + /PI +) cells were calculated. Stars indicate significant differences with parental PHFKs ($P<0.05$). Mean values of three independent experiments are presented as average/s.d. values. There is no significant difference between the E6/E7 and AA/E7 at passage 16, 30 or 65. The Student's *t*-test was used for statistical analysis.

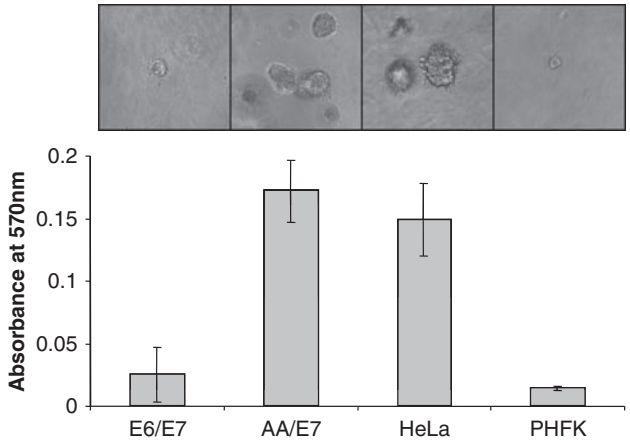

Figure 8 Colony formation assay in semi-soft agar. E6/E7 and AA/E7, as well as positive (HeLa) and negative control cells (parental PHFKs), were seeded in triplicate and grown in semi-soft agar for 10 days, as described in the Materials and methods. The top panel depicts (from left to right): E6/E7, AA/E7, HeLa and parental PHFKs. Cell proliferation was calculated as OD using the MTT assay. The average of three independent experiments is shown. Micrographs have all been taken with the same $\times 200$ magnification.

Table 1 Variation in spot detection between replicate 2D gels

Cell type	*Gel 1*	*Gel 2*	*Gel 3*	*Mean spot number*	*s.d.*	*% CV*
PHFK	360	405	383	383	18.37	3.32
AA/E7	369	377	399	382	12.68	2.75
E6/E7	359	384	371	371	10.21	4.80

Abbreviations: AA, Asian-American; CV, coefficient of variation; PHFK, primary human foreskin keratinocyte; 2D, two-dimensional.
Matched spots after editing are listed for each of three replicate gels containing protein from the parental keratinocytes and the keratinocyte cell lines immortalized with E6/E7 or AA/E7. The mean spot number is shown for each replicate set of three gels, along with the s.d. and the percent coefficient of variation (CV) for each set. Variation between the number of spots per gel is expressed as percent CV (% CV = 100 × (s.d./mean number of spots detected in gel set)). Student's *t*-test was performed on the normalized spot density values to find spots that were present in significantly different amounts at the 95% level of confidence in pair-wise comparisons between the AAE7/E6E7, the AAE7/PHFK and the E6E7/PHFK gel sets.

PHFKs. Five of these had not been reported earlier (14-3-3 protein zeta/delta, Ras-related protein Rab-30, protein DJ-1, transketolase and far upstream element-binding protein 1 (DNA helicase V)) and eight proteins revealed expression levels that were significantly different between the E6/E7 and AA/E7 gels (Table 2). These differentially expressed proteins are known to have metabolic functions in the cell (Table 2, Figure 9). Enzymes of amino acid metabolism and the tri-carboxylic acid cycle—cytoplasmic isocitrate dehydrogenase 1 (IDH1) as well as mitochondrial IDH2 and malate dehydrogenase-1—were all expressed to a lesser extent in the AA/E7 than the E6/E7 PHFKs. In contrast, glycolytic pathway enzymes—glyceraldehyde 3-phosphate dehydrogenase and pyruvate kinase M2—were found to be significantly increased in AA/E7 compared with E6/E7 PHFKs (Table 2, Figure 9). In addition, the protein SET (a nuclear oncogene), which is known to bind to glyceraldehyde 3-phosphate dehydrogenase (Carujo *et al*., 2006), was also expressed significantly higher in AA/E7 compared with E6/E7 PHFKs (Table 2, Figure 9). Finally, we observed a significant reduction in phosphoglucomutase-2 (regulatory enzyme in cellular glucose utilization) and the aldo-ketoreductase protein (AKR1C1) (a 20-α hydroxysteroid dehydrogenase involved in the reduction and elimination of progesterone) in AA/E7 compared with E6/E7 PHFKs (Table 2, Figure 9).

Discussion

We analyzed two common HPV16 strains, as defined by their E6 protein in cultured PHFKs. Our longitudinal cell culture studies investigating the immortalizing and transforming abilities of naturally occurring E6 variants in primary host cells of HPV are the first of their kind. Our results provide a mechanistic explanation for epidemiological studies reporting that the HPV16 E6 AA variant is up to 20-fold more prevalent than the E6 prototype in cervical cancer (Berumen *et al*., 2001).

AA/E7 showed faster growth and a dissimilar differentiation phenotype compared with E6/E7.

Table 2 Differentially expressed proteins in 2D gels

Spot number	*Gene ID*	*AC*	*Prot ID*	*Description*	*Avg ppm*	*Avg ppm*	*Avg ppm*	T-*test* P-*value*	T-*test* P-*value*	T-*test* P-*value*
					PHFK ± *s.d.*	*E6E7* ± *s.d.*	*AAE7* ± *s.d.*	*PHFK vs E6E7*	*PHFK vs AAE7*	*AAE7 vs E6E7*
109	YWHAZ	P63104	1433Z	14-3-3 protein zeta/delta	23284 ± 2816	11553 ± 2551	9827 ± 810	0.006	0.010	0.363
207 (1)	SET	Q01105	SET	Protein SET	226 ± 85	451 ± 60	714 ± 57	0.024	0.002	0.005
1001	RAB30	Q15771	RAB	Ras-related protein Rab-30	938 ± 98	394 ± 155	599 ± 169	0.011	0.053	0.197
3004	PARK7	Q99497	PARK7	Protein DJ-1	439 ± 176	916 ± 170	792 ± 132	0.028	0.054	0.376
4718 (2)	PGM2	Q96G03	PGM2	Phosphoglucomutase-2	487 ± 229	1151 ± 238	515 ± 157	0.025	0.871	0.024
5101 (3)	MDH1	P40925	MDHC	Malate dehydrogenase, cytoplasmic	1481 ± 418	2654 ± 229	1607 ± 354	0.022	0.711	0.018
5302 (4)	IDH1	O75874	IDHC	Isocitrate dehydrogenase (NADP)cytoplasmic	1589 ± 528	1256 ± 110	349 ± 229	0.389	0.039	0.010
6606	TKT	P29401	TKT	Transketolase	1220 ± 107	485 ± 164	689 ± 169	0.005	0.015	0.208
6703	FUBP1	Q96AE4	FUBP1	Far upstream element-binding protein1 (DNA helicase V)	0 ± 0	396 ± 117	475 ± 185	0.028	0.047	0.570
8218 (5)	AKR1C1	Q04828	AK1C1	Aldo-ketoreductase family 1 member C1	2332 ± 427	1632 ± 109	689 ± 86	0.097	0.018	0.0004
8304 (6)	IDH2	P48735	IDHP	Isocitrate dehydrogenase (NADP) mitochondrial	640 ± 170	997 ± 115	402 ± 90	0.047	0.121	0.003
8501 (7)	PKM2	P14618	KPYM	Pyruvate kinase isozymes M1/M2	15517 ± 2256	5906 ± 1861	11997 ± 2839	0.005	0.172	0.044
9103 (8)	GAPDH	P04406	G3P	Glyceraldehyde-3-phosphate dehydrogenase	12811 ± 2385	9292 ± 2797	17697 ± 1211	0.174	0.052	0.022

Abbreviations: AA, Asian-American; PHFK, primary human foreskin keratinocyte; ppm, parts per million; 2D, two-dimensional.
The eight proteins that were differentially expressed in E6/E7 and AA/E7 PHFKs are indicated in brackets in the first column to the left and are also marked in each of the three gels in Figure 9. The protein identities for each spot are listed. The other four columns to the left depict the proteins by means of gene identification (Gene ID), accession number (AC), protein identification (Prot ID) and description. Columns to the right depict average spot density values/s.d. across three replicate gels in ppm. Density values were normalized to the total density in each gel. Student's *t*-test (two-tail, 95% level of confidence) was calculated for pair-wise comparisons to identify proteins that were expressed at significantly different levels in parental PHFKs, PHFKs expressing E6/E7 or AA/E7 proteins. *T*-statistics indicating significantly different amounts of protein between the gel sets with a 95% confidence level are listed in the final three columns.

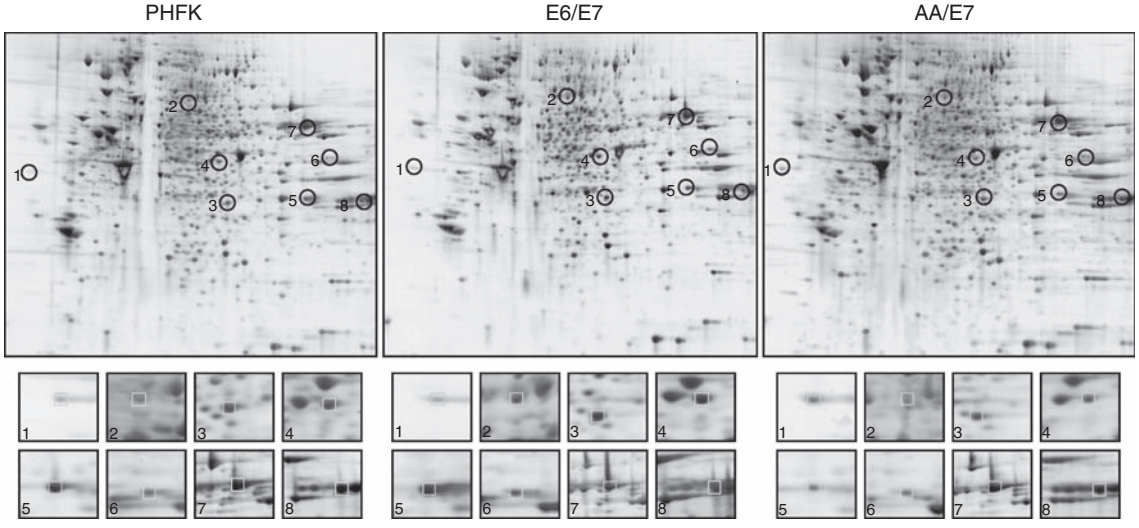

Figure 9 Differential protein expression using two-dimensional (2D) gel electrophoresis. Three independent 2D experiments were performed using *parental, E6/E7 and AA/E7 PHFKs*. One of the representative gels for each cell type is shown. Rows represent enlarged areas from one of the representative gels containing protein spots, named to the left of each row. Locations of protein spots in the 2D gels that are differentially expressed are shown ringed and numbered: Spot 1 corresponds to the SET protein, spot 2 corresponds to the phosphoglucomutase-2 (PGM2) protein, spot number 3 corresponds to malate dehydrogenase (MDH)1 protein, spot number 4 corresponds to the IDH1 protein, spot 5 corresponds to the AKR1C1 protein, spot number 6 corresponds to IDH2 protein, spot 7 corresponds to the pyruvate kinase M2 (PKM2) protein and spot 8 corresponds to the glyceraldehyde 3-phosphate dehydrogenase (GAPDH) protein. The different spot numbers are also marked in Table 2 in the first column to the left. Rows represent enlarged areas of gels containing protein spots, named to the left of each row. Cell type is listed above each column. Corresponding protein spots are marked with yellow squares in each row. A full colour version of this figure is available at the *Oncogene* journal online.

The thickness of the AA/E7 raft was approximately twice that of E6/E7. Only the AA/E7 culture showed a considerable portion of keratinized, atypical cells that were highly differentiated as defined by H + E and cytokeratin 10 staining, some of which co-expressed the early differentiation marker cytokeratin 5. In addition, a subset of the K10-positive keratinizing cells of the suprabasal compartment stained positive for Ki67 (Figure 4b), suggesting that AA/E7 is capable of inducing differentiation and proliferation in the same cell. The lack of detectable K10 in the presence of E6 prototype compared with certain E6 variants is not unprecedented and has previously been described by our group (Zehbe *et al*., 2009) using spontaneously immortalized keratinocytes, NIKS (Allen-Hoffmann *et al*., 2000).

Interestingly, K10 is not only a differentiation marker for suprabasal keratinocytes but also for reserve cell hyperplasia, immature squamous metaplasia and the cervical transformation zone (Maddox *et al*., 1999) wherein most cervical carcinomas arise. It has also been reported that cervical intraepithelial neoplasia can be divided into two subpopulations, one characterized by the reserve cell keratin phenotype (K10 positive) and the other by a keratin phenotype typical of non-keratinizing squamous epithelia (Smedts *et al*., 1993). In the same study, it was suggested that lesions with the former phenotype are progressive in nature, an observation that further supports the hypothesis that the AA variant is more tumorigenic than is the E6 prototype. Generally, keratinizing squamous cell carcinomas of the cervix often express more K10 than do non-keratinizing squamous cell tumors (Smedts *et al*., 1992). It remains to be analyzed whether keratinizing squamous cell carcinomas of HPV16-positive cancers express, to a higher extent, the AA variant than the E6 prototype.

Activities implicated in immortalization and transformation, such as p53 degradation were similar between E6/E7 and AA/E7 PHFKs, paralleling the observation in NIKS (Asadurian *et al*., 2007; Zehbe *et al*., 2009). hTERT induction (a measure of telomerase activity) was also comparable between prototype and variant E6 in this study. Instead, differences in the expression levels of several enzymes involved in metabolic activities were detected in E6/E7 and AA/E7 PHFKs.

Changes in cellular carbohydrate metabolism are a hallmark of malignant transformation and represent one of the earliest discernible events in tumorigenesis (Zwerschke *et al*., 2000). HPV oncoproteins have previously been shown to alter carbohydrate metabolism (Zwerschke *et al*., 2000; Mazurek *et al*., 2001). HPV16 E7 is shown to target the glycolytic control enzyme, pyruvate kinase M2 (a key player in reprogramming cellular carbohydrate metabolism in tumors), such that pyruvate kinase M2 is shifted to the tumor specific, dimeric form that possesses decreased substrate affinity (Mazurek *et al*., 2001). This study provides evidence that the E6 oncoprotein of HPV16 may have an additional role in modulating carbohydrate and other metabolic activities.

A striking observation from our studies was the decreased expression of IDH isoforms 1 and 2 in AA/E7 compared with E6/E7 PHFKs. IDH isoforms are rate-limiting enzymes, converting isocitrate into alpha-ketoglutarate in the mitochondria (IDH2, tri-carboxylic acid cycle) and in the cytosol (IDH1, amino acid metabolism). The tri-carboxylic acid cycle is subverted in many tumors and indeed all proliferating cells in favor of aerobic glycolysis, a phenomenon known as the Warburg effect (Vander Heiden *et al*., 2009). This effect is further reflected by the higher glyceraldehyde 3-phosphate dehydrogenase and pyruvate kinase M2 levels in AA/E7 compared with E6/E7 PHFKs and suggest enhanced aerobic glycolysis as an underlying mechanism for the higher immortalizing and transforming potential of AA/E7. Indeed, the Warburg effect has been reported to be essential for immortalization and transformation, as it renders cells resistant to oxidative stress and adaptive to hypoxia (Kondoh, 2008). Interestingly, disruption of an extra-mitochondrial process, characterized by reduced IDH1 activity and caused by tumor-associated mutations, has recently been reported for glioblastoma multiforme, a malignant brain tumor (Zhao *et al*., 2009). Reduced IDH1 activity leads to low levels of alpha-ketoglutarate in the cytosol and activation of hypoxia-induced factor, which promotes the transcription of genes functioning in energy metabolism, growth and differentiation (Pollard and Ratcliffe, 2009). A similar effect may hold true for some HPV-infected cells, albeit with a different underlying mechanism. Further study is required to determine the effects and causes of reduced levels of IDH1 in the AA/E7 line.

Reduced expression of the AKR1C1 in AA/E7 compared with E6/E7 PHFKs was another interesting observation. Reduced levels of AKR1C1 have been observed in breast cancer cell lines and paired tumor and normal tissue samples (Ji *et al*., 2004). The AKR1C isoforms control production of estrogens and androgens, therefore any deregulation in the levels or activity of these enzymes can alter the local hormone ratios in tissues and affect proliferation (Penning and Byrns, 2009). Reduced levels of the AKR1C1 in AA/E7 PHFKs may alter the local steroid hormone environment in infected cells to promote proliferation, a novel observation that merits further study.

In summary, HPV16 AA/E7 PHFKs reflect a phenotype more reminiscent of transformed cells than HPV16 E6/E7 PHFKs. Our studies suggest that AA/E7 may alter the regulation of the cellular energy generating system by differentially modulating metabolic enzymes and their associated pathways. These results introduce a new paradigm and warrant further studies on the mechanisms behind how primary human keratinocytes are immortalized and transformed into malignant tumors by viral oncoproteins of HPV16.

Materials and methods

Cell culture

PHFKs were obtained from Cell Applications, Inc. (San Diego, CA, USA) and sub-cultured using the recommended serum-free medium from the supplier. Cells were

grown without feeders throughout the study, as suggested by the supplier. When harvesting, trypsin-EDTA (Invitrogen, Burlington, ON, Canada) was used and inactivated with trypsin neutralizing solution, as recommended by the supplier (Cell Applications). Cells were passaged when they reached 80% confluency and were counted with a Coulter counter after each passage. Throughout the study, 125 000 cells were re-plated after trypsinization.

Retroviral transduction
The HPV16 E7 gene, the E6 gene from prototype (E6) or the Q14H/H78Y/L83V AA variant were separately cloned into the pLXSN retroviral vector and used to transfect Phoenix helper cells by calcium phosphate precipitation (Clonetech, Heidelberg, Germany) as previously described (Zehbe *et al*., 2009). After 48 h, the viral supernatant (in the presence of polybrene (1 μg/ml)) was used to infect (for 3 h) passage 3 PHFK cultures: empty vector, E6 and E7 (E6/E7), or AA and E7 (AA/E7). Transductions were performed in triplicate. To avoid supernatant serum-induced differentiation, serum-free keratinocyte medium (Cell Applications) was then added 1:1 and maintained for a further 12 h. For stable transduction, PHFKs were kept in keratinocyte medium for 48 h and were thereafter selected with 100 μg/ml G418. Resistant clones in the Petri dishes were pooled and further grown as mass cultures.

Quantitative real-time PCR
Total RNA from the various cell clones was extracted using the RNAqueous kit from Ambion (Applied Biosystems (ABI), Foster City, CA, USA), integrity-tested/quantified using the Experion Automated Electrophoresis system (Bio-Rad, Mississauga, ON, CA), and reverse-transcribed using the high-capacity complementary DNA Archive kit (ABI), as described (DeCarlo *et al*., 2008). For HPV16 E6, E7 (assay on demand), hTERT, and the housekeeping gene HPRT1, TaqMan primers were obtained from ABI. Quantitative reverse transcriptase–PCR using TaqMan chemistry was performed in triplicate using a 7500 ABI cycler, as described (DeCarlo *et al*., 2008).

Western blot
To determine the levels of p53, p16 or actin in each of the keratinocyte lines, cells were trypsinized and subsequently lysed in ice-cold lysis buffer (10 mM Tris, pH 8.0, 0.25 M sucrose, 0.2 M NaCl, 2 mM $MgCl_2$, 1 mM $CaCl_2$, 1% Triton X-100 and 1 mM phenylmethylsulphonyl fluoride) for 20 min and centrifuged at 14 000 revolutions per minute for 20 min at 4 °C in a microcentrifuge. Between 30–50 ug of protein lysate was loaded in each lane of a 12% sodium dodecyl sulfate–polyacrylamide gel, electrophoresed, transferred onto a polyvinylidene difluoride membrane (Millipore, Kingston, ON, Canada), and immunoblotted with either mouse anti-p53 (clone DO-7, DAKO, Mississauga, ON, Canada), mouse anti-p16 (MTM Laboratories, Heidelberg, Germany) or goat anti-actin (sc-1616, Santa Cruz Biotechnologies, Heidelberg, Germany) at a dilution of 1:1000. Detection was achieved using the ECL Plus Western Detection Kit (Amersham, Piscataway, NJ, USA).

Flow cytometry
Cell cycle analysis was performed after incubating the AA/E7, E6/E7 or vector alone PHFKs in 0.5 nM AD for 24 h. The cells were fixed in cold 75% ethanol overnight. The fixed cells were washed with phosphate-buffered saline, then incubated in phosphate-buffered saline containing RNase (50 μg/ml) and propidium iodide (5 μg/ml) and the suspension was analyzed by flow cytometry on a FACSCalibur flow cytometer (Becton Dickinson, Mississauga, ON, Canada).

Apoptosis was induced by maintaining the PHFKs in semi-solid medium for 24 h, as described previously (Zehbe *et al*., 2009). Cells were washed three times with phosphate-buffered saline, then analyzed by flow cytometry using the annexin V-FITC assay (Sigma, Oakville, ON, Canada).

Organotypic raft cultures and immunofluorescence
Raft cultures derived from E6/E7 and AA/E7 PHFKs were grown in triplicate, as described (Zehbe *et al*., 2009). Immunofluorescence on raft culture sections was performed using the appropriate primary antibodies—a rabbit anti-K5 polyclonal antibody (#24647, Abcam, Cambridge, MA, USA), a mouse anti-K10 monoclonal antibody or a mouse anti-Ki67 (both from DAKO)—followed by secondary antibodies—AlexaFluor 488 donkey anti-rabbit or AlexaFluor 594 donkey anti-mouse—as described (Zehbe *et al*., 2009). Ki67 was detected using a peroxidase-based reporter molecule system as described (Zehbe *et al*., 1999).

Transformation in vitro *assay*
Keratinocyte cultures from passage 65, as well as negative and positive control cells (parental PHFKs from passage 3 and HeLa cells, respectively), were assessed for their ability to form colonies in semi-soft agar using the CytoSelect 96-well Cell Transformation Kit (Cell Biolabs, Inc., Burlington, ON, Canada). Five thousand cells per well were seeded in triplicate in a 96-well plate. After 10 days, colony formation was documented microscopically, then the agar was solubilized and the cells lysed, as recommended by the supplier. MTT assay was then performed to quantify cell viability (yellow tetrazole is reduced to purple formazan in the mitochondria of living cells). This product was dissolved in sodium dodecyl sulfate (provided in the transformation kit) to produce a colored solution, which was then measured at 570 nm by a microtiter spectrophotometer (BioTek, Nepean, ON, Canada).

Two-dimensional gel electrophoresis, matrix-assisted laser desorption/ionization and mass spectrometry
Protein samples (60 μg) were focused on 11 cm, immobilized, linear pH gradient (pH 3-10) strip gels (Bio-Rad Laboratories) for a total of 35 000 VHr at 8000 V. Second dimension electrophoresis was carried out using 10% sodium dodecyl sulfate–polyacrylamide gel electrophoresis. Gels were stained overnight in SYPRO Ruby protein gel stain (Bio-Rad Laboratories) and scanned on a FX Molecular Imager instrument at 50 μm resolution (Bio-Rad Laboratories). Scanned images of gels were analyzed using PD Quest Advanced v. 8.0 software (Bio-Rad Laboratories).

In-gel trypsin digestion and generation of peptide spectra by matrix-assisted laser desorption/ionization were performed as described previously, with some modifications (Naryzhny and Lee, 2007). The produced peptides were collected directly from the gel plug digest, mixed (1:1) with α-cyano-4-hydroxycinnamic acid matrix solution (Fluka, Buchs, Switzerland), 10 mg/ml, in 50% acetonitrile, 20% ethanol, 0.01% trifluoroacetic acid, applied to the target plate, crystallized and analyzed by matrix-assisted laser desorption/ionization on a Micro MX instrument (Waters Inc., Milford, MA, USA). Spectra were acquired in positive reflection mode (1100–3000 Da mass range) using a total of 150 shots in a random pattern across the spotted sample, and were processed using MassLynx Global version 4.0 software (Waters Inc.). Peak lists

were obtained from raw data after smoothing, background subtraction and data centroiding. Internal calibration was carried out using trypsin-autolysis fragments at 1045.5642 and 2211.1046 Da. Peptide mass fingerprinting analysis was carried out using Aldente (http://ca.expasy.org/tools), or MasScot (http://www.matrixscience.com) software programs. The protein databases searched using Aldente were UniProtKB/Swiss-Prot release 56.9 of 03 March 2009 and UniProtKB/TrEMBL release 39.9 of 03 March 2009. The databases searched using MASCOT were MSDB 20060831, SwissProt 57.2 and NCBInr 20090606. Searches were limited to the taxon *Homo sapiens* and single positive charge ions, with modifications to cysteine residues and single missed cleavages accounted for. Significant matches recovered using the Aldente software showed scores >15.0. Confirmation of protein identities was performed using the MasScot software. Spots with intensities below 200 parts per million were considered below the limits of detection. In the PD Quest spot analysis, one of the AA/E7 gels was selected as the 'master' to which the other gels were compared. Spots were added to the master gel from the other gels if they were present in at least one of the three gels in each set.

Statistical analysis

Cell culture data were analyzed by the Wilcoxon signed-rank test or the Fisher's exact test. Data from biochemical assays and two-dimensional gel electrophoresis were calculated using the two-tailed Student's *t*-test. Differences were considered significant at $P<0.05$.

Conflict of interest

The authors declare no conflict of interest.

Acknowledgements

We are grateful to the staff from the Central Laboratory of the Thunder Bay Regional Health Sciences Centre for technical assistance and Bruce Weaver from the Northern School of Medicine, West-Campus, Thunder Bay for help with statistical analysis. This work was funded by a Discovery Grant to IZ from the Natural Sciences and Engineering Research Council of Canada (NSERC).

References

Allen-Hoffmann BL, Schlosser SJ, Ivarie CA, Sattler CA, Meisner LF, O'Connor SL. (2000). Normal growth and differentiation in a spontaneously immortalized near-diploid human keratinocyte cell line, NIKS. *J Invest Dermatol* **114**: 444–455.

Androphy EJ, Schiller JT, Lowy DR. (1985). Identification of the protein encoded by the E6 transforming gene of bovine papillomavirus. *Science* **230**: 442–445.

Asadurian Y, Kurilin H, Lichtig H, Jackman A, Gonen P, Tommasino M *et al*. (2007). Activities of human papillomavirus 16 E6 natural variants in human keratinocytes. *J Med Virol* **79**: 1751–1760.

Bernard HU. (2005). The clinical importance of the nomenclature, evolution and taxonomy of human papillomaviruses. *J Clin Virol* **32**(Suppl 1): S1–S6.

Bernard HU, Calleja-Macias IE, Dunn ST. (2006). Genome variation of human papillomavirus types: phylogenetic and medical implications. *Int J Cancer* **118**: 1071–1076.

Berumen J, Ordonez RM, Lazcano E, Salmeron J, Galvan SC, Estrada RA *et al*. (2001). Asian-American variants of human papillomavirus 16 and risk for cervical cancer: a case-control study. *J Natl Cancer Inst* **93**: 1325–1330.

Boukamp P, Petrussevska RT, Breitkreutz D, Hornung J, Markham A, Fusenig NE. (1988). Normal keratinization in a spontaneously immortalized aneuploid human keratinocyte cell line. *J Cell Biol* **106**: 761–771.

Camus S, Menendez S, Cheok CF, Stevenson LF, Lain S, Lane DP. (2007). Ubi-independent degradation of p53 mediated by high-risk human papillomavirus protein E6. *Oncogene* **26**: 4059–4070.

Carujo S, Estanyol JM, Ejarque A, Agell N, Bachs O, Pujol MJ. (2006). Glyceraldehyde 3-phosphate dehydrogenase is a SET-binding protein and regulates cyclin B-cdk1 activity. *Oncogene* **25**: 4033–4042.

Castellsague X. (2008). Natural history and epidemiology of HPV infection and cervical cancer. *Gynecol Oncol* **110**: S4–S7.

Chakrabarti O, Veeraraghavalu K, Tergaonkar V, Liu Y, Androphy EJ, Stanley MA *et al*. (2004). Human papillomavirus type 16 E6 amino acid 83 variants enhance E6-mediated MAPK signaling and differentially regulate tumorigenesis by notch signaling and oncogenic Ras. *J Virol* **78**: 5934–5945.

Chen Z, Terai M, Fu L, Herrero R, DeSalle R, Burk RD. (2005). Diversifying selection in human papillomavirus type 16 lineages based on complete genome analyses. *J Virol* **79**: 7014–7023.

Dalal S, Gao Q, Androphy EJ, Band V. (1996). Mutational analysis of human papillomavirus type 16 E6 demonstrates that p53 degradation is necessary for immortalization of mammary epithelial cells. *J Virol* **70**: 683–688.

de Araujo Souza PS, Sichero L, Maciaq PC. (2009). HPV variants and HLA polymorphisms: the role of variability on the risk of cervical cancer. *Future Oncol* **5**: 359–370.

DeCarlo CA, Escott NG, Werner J, Robinson K, Lambert PF, Law RD *et al*. (2008). Gene expression analysis of interferon kappa in laser capture microdissected cervical epithelium. *Anal Biochem* **381**: 59–66.

Fu B, Quintero J, Baker CC. (2003). Keratinocyte growth conditions modulate telomerase expression, senescence, and immortalization by human papillomavirus type 16 E6 and E7 oncogenes. *Cancer Res* **63**: 7815–7824.

Grodzki M, Besson G, Clavel C, Arslan A, Franceschi S, Birembaut P *et al*. (2006). Increased risk for cervical disease progression of French women infected with the human papillomavirus type 16 E6-350G variant. *Cancer Epidemiol Biomarkers Prev* **15**: 820–822.

Hahn WC, Counter CM, Lundberg AS, Beijersbergen RL, Brooks MW, Weinberg RA. (1999). Creation of human tumour cells with defined genetic elements. *Nature* **400**: 464–468.

Hanahan D, Weinberg RA. The hallmarks of cancer (2000). *Cell* **100**: 57–70.

Huibregtse JM, Scheffner M, Howley PM. (1991). A cellular protein mediates association of p53 with the E6 oncoprotein of human papillomavirus types 16 or 18. *EMBO J* **10**: 4129–4135.

James MA, Lee JH, Klingelhutz AJ. (2006). HPV16-E6 associated hTERT promoter acetylation is E6AP dependent, increased in later passage cells and enhanced by loss of p300. *Int J Cancer* **119**: 1878–1885.

Ji Q, Aoyama C, Nien YD, Liu P, Chen P, Chang L *et al*. (2004). Selective loss of AKR1C1 and AKR1C2 in breast cancer and their potential effect on progesterone signaling. *Cancer Res* **64**: 7610–7617.

Kammer C, Tommasino M, Syrjanen S, Delius H, Hebling U, Warthorst U *et al*. (2002). Variants of the long control region and the E6 oncogene in European human papillomavirus type 16 isolates: implications for cervical disease. *Br J Cancer* **86**: 269–273.

Kaur P, McDougall JK. (1989). HPV-18 immortalization of human keratinocytes. *Virology* **173**: 302–310.

Kirkpatrick KL, Newbold RF, Mokbel K. (2004). The mRNA expression of hTERT in human breast carcinomas correlates with VEGF expression. *J Carcinog* **3**: 1.

Klingelhutz AJ, Foster SA, McDougall JK. (1996). Telomerase activation by the E6 gene product of human papillomavirus type 16. *Nature* **380**: 79–82.

Kondoh H. (2008). Cellular life span and the Warburg effect. *Exp Cell Res* **314**: 1923–1928.

Kyo S, Kanaya T, Takakura M, Tanaka M, Inoue M. (1999). Human telomerase reverse transcriptase as a critical determinant of telomerase activity in normal and malignant endometrial tissues. *Int J Cancer* **80**: 60–63.

Lee K, Magalhaes I, Clavel C, Briolat J, Birembaut P, Tommasino M *et al*. (2008). Human papillomavirus 16 E6, L1, L2 and E2 gene variants in cervical lesion progression. *Virus Res* **131**: 106–110.

Lichtig H, Algrisi M, Botzer LE, Abadi T, Verbitzky Y, Jackman A *et al*. (2006). HPV16 E6 natural variants exhibit different activities in functional assays relevant to the carcinogenic potential of E6. *Virology* **350**: 216–227.

Maddox P, Sasieni P, Szarewski A, Anderson M, Hanby A. (1999). Differential expression of keratins 10, 17, and 19 in normal cervical epithelium, cervical intraepithelial neoplasia, and cervical carcinoma. *J Clin Pathol* **52**: 41–46.

Marconi A, Atzei P, Panza C, Fila C, Tiberio R, Truzzi F *et al*. (2004). FLICE/caspase-8 activation triggers anoikis induced by beta1-integrin blockade in human keratinocytes. *J Cell Sci* **117**: 5815–5823.

Mazurek S, Zwerschke W, Jansen-Durr P, Eigenbrodt E. (2001). Effects of the human papillomavirus HPV16-E7 oncoprotein on glycolysis and glutaminolysis: role of pyruvate kinase type M2 and the glycolytic-enzyme complex. *Biochem J* **356**: 247–256.

McMurray HR, McCance DJ. (2004). Degradation of p53, not telomerase activation, by E6 is required for bypass of crisis and immortalization by human papillomavirus type 16 E6/E7. *J Virol* **78**: 5698–5706.

Naryzhny SN, Lee H. (2007). Characterization of proliferating cell nuclear antigen (PCNA) isoforms in normal and cancer cells: there is no cancer-associated form of PCNA. *FEBS Lett* **581**: 4917–4920.

Nomine Y, Masson M, Charbonnier S, Zanier K, Ristriani T, Deryckere F *et al*. (2006). Structural and functional analysis of E6 oncoprotein: insights in the molecular pathways of human papillomavirus-mediated pathogenesis. *Mol Cell* **21**: 665–678.

Pollard PJ, Ratcliffe PJ. (2009). Puzzling patterns of predisposition. *Science* **324**: 192–194.

Penning T, Byrns M. (2009). Steroid hormone transforming aldo-ketoreductases and cancer. *Ann NY Acad Sci* **1155**: 33–42.

Scheffner M, Huibregtse JM, Vierstra RD, Howley PM. (1993). The HPV-16 E6 and E6-AP complex functions as a ubiquitin-protein ligase in the ubiquitination of p53. *Cell* **75**: 495–505.

Schonk DM, Kuijpers HJ, van Drunen E, van Dalen CH, Geurts van Kessel AH, Verheijen R *et al*. (1989). Assignment of the gene(s) involved in the expression of the proliferation-related Ki-67 antigen to human chromosome 10. *Hum Genet* **83**: 297–299.

Seedorf K, Krammer G, Durst M, Subai S, Rowekamp WG. (1985). Human papillomavirus type 16 DNA sequence. *Virology* **145**: 181–185.

Sekaric P, Cherry JJ, Androphy EJ. (2008). Binding of human papillomavirus type 16 E6 to E6AP is not required for activation of hTERT. *J Virol* **82**: 71–76.

Shamanin VA, Sekaric P, Androphy EJ. (2008). hAda3 degradation by papillomavirus type 16 E6 correlates with abrogation of the p14ARF-p53 pathway and efficient immortalization of human mammary epithelial cells. *J Virology* **82**: 3912–3920.

Shen ZY, Xu LY, Li EM, Cai WJ, Shen J, Chen MH *et al*. (2004). The multistage process of carcinogenesis in human esophageal epithelial cells induced by human papillomavirus. *Oncol Rep* **11**: 647–654.

Smedts F, Ramaekers F, Troyanovsky S, Pruszczynski M, Link M, Lane B *et al*. (1992). Keratin expression in cervical cancer. *Am J Pathol* **141**: 497–511.

Smedts F, Ramaekers FC, Vooijs PG. (1993). The dynamics of keratin expression in malignant transformation of cervical epithelium: a review. *Obstet Gynecol* **82**: 465.

Song S, Gulliver GA, Lambert PF. (1998). Human papillomavirus type 16 E6 and E7 oncogenes abrogate radiation-induced DNA damage responses *in vivo* through p53-dependent and p53-independent pathways. *Proc Natl Acad Sci USA* **95**: 2290–2295.

Sprague DL, Phillips SL, Mitchell CJ, Berger KL, Lace M, Turek LP *et al*. (2002). Telomerase activation in cervical keratinocytes containing stably replicating human papillomavirus type 16 episomes. *Virology* **301**: 247–254.

Stöppler MC, Ching K, Stöppler H, Clancy K, Schlegel R, Icenogle J. (1996). Natural variants of the human papillomavirus type 16 E6 protein differ in their abilities to alter keratinocyte differentiation and to induce p53 degradation. *J Virol* **70**: 6987–6993.

Sumida T, Hamakawa H, Sogawa K, Sugita A, Tanioka H, Ueda N. (1999). Telomerase components as a diagnostic tool in human oral lesions. *Int J Cancer* **80**: 1–4.

Tidy JA, Vousden KH, Farrell PJ. (1989). Relation between infection with a subtype of HPV16 and cervical neoplasia. *Lancet* **8649**: 1225–1227.

Vander Heiden MG, Cantley LC, Thompson CB. (2009). Understanding the Warburg effect: the metabolic requirements of cell proliferation. *Science* **324**: 1029–1033.

Woodworth CD, Bowden PE, Doniger J, Pirisi L, Barnes W, Lancaster WD *et al*. (1988). Characterization of normal human exocervical epithelial cells immortalized *in vitro* by papillomavirus types 16 and 18 DNA. *Cancer Res* **48**: 4620–4628.

Xi LF, Koutsky LA, Galloway DA, Kuypers J, Hughes JP, Wheeler CM *et al*. (1997). Genomic variation of human papillomavirus type 16 and risk for high grade cervical intraepithelial neoplasia. *J Natl Cancer Inst* **89**: 796–802.

Xi LF, Critchlow CW, Wheeler CM, Koutsky LA, Galloway DA, Kuypers J *et al*. (1998). Risk of anal carcinoma in situ in relation to human papillomavirus type 16 variants. *Cancer Res* **58**: 3839–3844.

Xi LF, Kiviat NB, Hildesheim A, Galloway DA, Wheeler CM, Ho J *et al*. (2006). Human papillomavirus type 16 and 18 variants: race-related distribution and persistence. *J Natl Cancer Inst* **98**: 1045–1052.

Xi LF, Koutsky LA, Hildesheim A, Galloway DA, Wheeler CM, Winer RL *et al*. (2007). Risk for high-grade cervical intraepithelial neoplasia associated with variants of human papillomavirus types 16 and 18. *Cancer Epidemiol Biomarkers Prev* **16**: 4–10.

Zhao S, Lin Y, Xu W, Jiang W, Zha Z, Wang P *et al*. (2009). Glioma-derived mutations in IDH1 dominantly inhibit IDH1 catalytic activity and induce HIF-1alpha. *Science* **324**: 261–265.

Zehbe I, Wilander E, Delius H, Tommasino M. (1998a). Human papillomavirus 16 E6 variants are more prevalent in invasive cervical carcinoma than the prototype. *Cancer Res* **58**: 829–833.

Zehbe I, Voglino G, Delius H, Wilander E, Tommasino M. (1998b). Risk of cervical cancer and geographical variations of human papillomavirus 16 E6 polymorphisms. *Lancet* **352**: 1441–1442.

Zehbe I, Rätsch A, Alunni-Fabbroni M, Burzlaff A, Bakos E, Dürst M *et al*. (1999). Overriding of cyclin-dependent kinase inhibitors by high and low risk human papillomavirus types: evidence for an *in vivo* role in cervical lesions. *Oncogene* **18**: 2201–2211.

Zehbe I, Tachezy R, Mytilineos J, Voglino G, Mikyskova I, Delius H *et al*. (2001). Human papillomavirus 16 E6 polymorphisms in cervical lesions from different European populations and their correlation with human leukocyte antigen class II haplotypes. *Int J Cancer* **94**: 711–716.

Zehbe I, Mytilineos J, Wikstrom I, Henriksen R, Edler L, Tommasino M. (2003). Association between human papillomavirus 16 E6 variants and human leukocyte antigen class I polymorphism in cervical cancer of Swedish women. *Hum Immunol* **64**: 538–542.

Zehbe I, Richard C, DeCarlo CA, Shai A, Lambert PF, Lichtig H *et al*. (2009). Human papillomavirus 16 E6 variants differ in their dysregulation of human keratinocyte differentiation and apoptosis. *Virology* **383**: 69–77.

Zwerschke W, Mannhardt B, Massimi P, Nauenburg S, Pim D, Nickel W *et al*. (2000). Allosteric activation of acid α-glucosidase by the human papillomavirus E7 protein. *J Biol Chem* **275**: 9534–9541.